Inorg. Chem. **2006**, *45*, 10293–10299

A Chelate-Stabilized Ruthenium(σ-pyrrolato) Complex: Resolving Ambiguities in Nuclearity and Coordination Geometry through ^{1}H PGSE and ^{31}P Solid-State NMR Studies

Heather M. Foucault, David L. Bryce,* and Deryn E. Fogg*

Center for Catalysis Research and Innovation, Department of Chemistry, University of Ottawa, Ottawa, Ontario, Canada K1N 6N5

Received June 8, 2006

Reaction of $RuCl_2(PPh_3)_3$ with LiNN′ (NN′ = 2-[(2,6-diisopropylphenyl)imino]pyrrolide) affords a single product, with the empirical formula $RuCl[(2,6\text{-}^iPr_2C_6H_3)N{=}CHC_4H_3N](PPh_3)_2$. We identify this species as a σ-pyrrolato complex, $[Ru(NN')(PPh_3)_2]_2(\mu\text{-}Cl)_2$ (**3b**), rather than mononuclear $RuCl(NN')(PPh_3)_2$ (**3a**), on the basis of detailed 1D and 2D NMR characterization in solution and in the solid state. Retention of the chelating, σ-bound iminopyrrolato unit within **3b**, despite the presence of labile (dative) chloride and PPh_3 donors, indicates that the chelate effect is sufficient to inhibit $\sigma \rightarrow \pi$ isomerization of **3b** to a piano-stool, π-pyrrolato structure. 2D COSY, SECSY, and *J*-resolved solid-state ^{31}P NMR experiments confirm that the PPh_3 ligands on each metal center are magnetically and crystallographically inequivalent, and ^{31}P CP/MAS NMR experiments reveal the largest ^{99}Ru–^{31}P spin–spin coupling constant ($^1J(^{99}Ru,^{31}P) = 244 \pm 20$ Hz) yet measured. Finally, ^{31}P dipolar-chemical shift spectroscopy is applied to determine benchmark phosphorus chemical shift tensors for phosphine ligands in hexacoordinate ruthenium complexes.

Introduction

As part of an ongoing investigation into the utility of pseudohalide ligands in Ru-catalyzed olefin metathesis,[1] we recently reported examples of catalysts containing an N-anionic donor.[2] Iminopyrrolato complexes $RuCl(NN')(L_n)(=CHPh)$ (Chart 1: **1a**, $L_n = PCy_3$; **1b**, $L_n = (py)_2$; NN′ = 2-[(2,6-^{i}Pr$_2$C$_6$H$_3$)N=CH]C$_4$H$_3$N; py = pyridine) promoted ring-closing and ring-opening metathesis reactions at 70 °C in air. These complexes were designed as probe systems enabling convenient preliminary assay of Ru−pyrrolide systems in metathesis, rather than as targets in their own right: their activity is limited by the absence of a strongly donating neutral ligand in the metathesis-active intermediate (as opposed to the precatalyst, the PCy_3 ligand in **1a** serving only as a placeholder for incoming olefin).[1c] This is compounded by the low lability of the PCy_3 and, more unexpectedly, the pyridine ligands. Prior to embarking on synthesis of potentially more activating pyrrolide-based ligand sets, however, we wished to examine the possibility of limitations arising from $\sigma \rightarrow \pi$ isomerization of the heterocyclic pyrrolide ring. The unsupported pyrrolide anion exhibits preferential π-coordination to ruthenium, as exemplified by the piano-stool complexes $RuX(\eta^5\text{-}C_5H_4N)(PPh_3)_2$ (**2a**, X = Cl; **2b**, X = H).[3] We have been able to restrain a similar tendency toward π-coordination of aryloxide ligands through incorporation of these anionic donors into a five- or six-membered[4] (but not a seven-membered)[5] chelate ring.

Chart 1

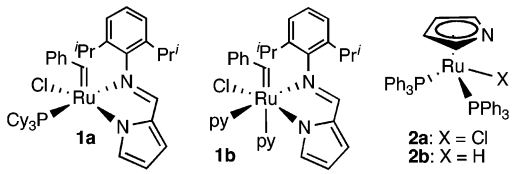

* To whom correspondence should be addressed. E-mail: dfogg@uottawa.ca (D.E.F.); dbryce@uottawa.ca (D.L.B.). Fax: (613) 562-5170.

(1) (a) Conrad, J. C.; Parnas, H. H.; Snelgrove, J. L.; Fogg, D. E. *J. Am. Chem. Soc.* **2005**, *127*, 11882−11883. (b) Conrad, J. C.; Amoroso, D.; Czechura, P.; Yap, G. P. A.; Fogg, D. E. *Organometallics* **2003**, *22*, 3634−3636. (c) Conrad, J. C.; Fogg, D. E. *Curr. Org. Chem.* **2006**, *10*, 185−202 and references therein.

(2) Drouin, S. D.; Foucault, H. M.; Yap, G. P. A.; Fogg, D. E. *Can. J. Chem.* **2005**, *83*, 748−754.

(3) Rakowski DuBois, M.; Parker, K. G.; Ohman, C.; Noll, B. C. *Organometallics* **1997**, *16*, 2325−2334.

(4) Monfette, S.; Fogg, D. E. *Organometallics* **2006**, *25*, 1940−1944.

(5) Snelgrove, J. L.; Conrad, J. C.; Eelman, M. D.; Moriarty, M. M.; Yap, G. P. A.; Fogg, D. E. *Organometallics* **2005**, *24*, 103−109.

10.1021/ic061021i CCC: $33.50
Published on Web 11/16/2006

While **1a**/**b** likewise appear to be resistant to isomerization, it is unclear whether this reflects the inherent stability of the chelate ring (the potential hemilability of which is suggested by discussions of related Schiff base complexes)[6] or the relatively low lability of the phosphine or pyridine donors, loss of which is a prerequisite for $\sigma \rightarrow \pi$ isomerization, as well as metathesis.[1c] To clarify the isomerization tendencies of the iminopyrrolato ligand within an unequivocally labile environment by direct comparison with the behavior of pyrrolide,[3] we undertook examination of the reaction of $RuCl_2(PPh_3)_3$ with lithium iminopyrrolide. This reaction is designed to probe the preferred coordination properties of the pyrrolide ligand within a five-membered chelate ring: that is, to evaluate the utility of the pyrrolide donor as an N-based pseudohalide ligand. (The Schiff base "end" of the ligand serves only as a convenient neutral donor for the purposes of this study). Here we describe the resulting formation of a κ^2-*N*,*N*′-pyrrolide complex with empirical formula $RuCl[(2,6\text{-}^iPr_2C_6H_3)N{=}CHC_4H_3N](PPh_3)_2$. Analysis by MALDI mass spectrometry, 2D correlation NMR experiments, and pulsed field gradient spin−echo (PGSE) diffusion NMR measurements provided considerable insight into the molecular structure of the complex but was inconclusive as to the absolute ligand orientation. We therefore turned to solid-state NMR analysis in order to clarify these details. These studies enable us to identify the product as $[Ru(NN')(PPh_3)_2]_2(\mu\text{-}Cl)_2$ (**3b**). The stability of **3b**, despite the presence of labile PPh_3 and edge-bridging, dative chloride donors, provides strong evidence for the stability of the chelated iminopyrrolide unit against $\sigma \rightarrow \pi$ isomerization.

The solid-state NMR study provided important fundamental information on the orientation-dependent second-rank ^{31}P NMR interaction tensors (e.g., chemical shift, dipolar (*D*), and indirect nuclear spin−spin coupling (*J*)). Although ^{31}P solid-state NMR studies aimed at evaluation of such parameters have been undertaken on metal−phosphine complexes of chromium,[7,8] molybdenum,[7,9] tungsten,[7,9a] manganese,[9a] cobalt,[10] rhodium,[11] iridium,[11f,12] nickel,[7,13] palladium,[7,14] platinum,[7,12,15] copper,[16] silver,[16i,17] gold,[11f,16b,18] and mercury,[17b,19] few such studies have been undertaken on ruthenium phosphine complexes.[11f,20] Indeed, the first measurements of the principal components of the phosphorus chemical shift tensor for an octahedral ruthenium complex were reported by Eichele and co-workers only in 2004.[20d] 1D and 2D ^{31}P solid-state NMR data obtained from magic-angle-spinning (MAS) and stationary samples of **3b** thus have additional value in establishing some benchmark ^{31}P NMR parameters for phosphine ligands in hexacoordinate ruthenium complexes.

(6) Opstal, T.; Couchez, K.; Verpoort, F. *Adv. Synth. Catal.* **2003**, *345*, 393−401.

(7) Eichele, K.; Wasylishen, R. E.; Kessler, J. M.; Solujic, L.; Nelson, J. H. *Inorg. Chem.* **1996**, *35*, 3904−3912.

(8) Huang, Y.; Uhm, H. L.; Gilson, D. F. R.; Butler, I. S. *Inorg. Chem.* **1997**, *36*, 435−438.

(9) (a) Eichele, K.; Wasylishen, R. E.; Nelson, J. H. *J. Phys. Chem. A* **1997**, *101*, 5463−5468. (b) Lindner, E.; Fawzi, R.; Mayer, H. A.; Eichele, K.; Pohmer, K. *Inorg. Chem.* **1991**, *30*, 1102−1107. (c) Eichele, K.; Wasylishen, R. E.; Maitra, K.; Nelson, J. H.; Britten, J. F. *Inorg. Chem.* **1997**, *36*, 3539−3544. (d) Wosnick, J. H.; Morin, F. G.; Gilson, D. F. R. *Can. J. Chem.* **1998**, *76*, 1280−1283. (e) Eichele, K.; Ossenkamp, G. C.; Wasylishen, R. E.; Cameron, T. S. *Inorg. Chem.* **1999**, *38*, 639−651.

(10) (a) Schurko, R. W.; Wasylishen, R. E.; Moore, S. J.; Marzilli, L. G.; Nelson, J. H. *Can. J. Chem.* **1999**, *77*, 1973−1983. (b) Szalontai, G. *Monatsh. Chem.* **2002**, *133*, 1575−1586.

(11) (a) Wu, G.; Wasylishen, R. E.; Curtis, R. D. *Can. J. Chem.* **1992**, *70*, 863−869. (b) Wu, G.; Wasylishen, R. E. *Inorg. Chem.* **1992**, *31*, 145−148. (c) Naito, A.; Sastry, D. L.; McDowell, C. A. *Chem. Phys. Lett.* **1985**, *115*, 19−23. (d) Wu, G.; Wasylishen, R. E. *Organometallics* **1992**, *11*, 3242−3248. (e) Szalontai, G.; Bakos, J.; Aime, S.; Gobetto, R. *J. Organomet. Chem.* **1993**, *463*, 223−226. (f) Albinati, A.; Eckert, J.; Hofmann, P.; Ruegger, H.; Venanzi, L. M. *Inorg. Chem.* **1993**, *32*, 2377−2390.

(12) Wu, G.; Wasylishen, R. E. *Inorg. Chem.* **1994**, *33*, 2774−2778.

(13) Christendat, D.; Butler, I. S.; Gilson, D. F. R.; Hynes, R.; Morin, F. G. *Inorg. Chim. Acta* **2004**, *357*, 3775−3779.

(14) Ruegger, H. *Magn. Reson. Chem.* **2004**, *42*, 814−818.

(15) (a) Power, W. P.; Wasylishen, R. E. *Inorg. Chem.* **1992**, *31*, 1, 2176−2183. (b) Bechmann, M.; Dusold, S.; Geipel, F.; Sebald, A.; Sellmann, D. *J. Phys. Chem. A* **2005**, *109*, 5275−5280. (c) Kourkine, I. V.; Chapman, M. B.; Glueck, D. S.; Eichele, K.; Wasylishen, R. E.; Yap, G. P. A.; Liable-Sands, L. M.; Rheingold, A. L. *Inorg. Chem.* **1996**, *35*, 1478−1485.

(16) (a) Bowmaker, G. A.; Cotton, J. D.; Healy, P. C.; Kildea, J. D.; Silong, S. B.; Skelton, B. W.; White, A. H. *Inorg. Chem.* **1989**, *28*, 1462−1466. (b) Berners-Price, S. J.; Colquhoun, L. A.; Healy, P. C.; Byriel, K. A.; Hanna, J. V. *J. Chem. Soc., Dalton Trans.* **1992**, 3357−3363. (c) Hanna, J. V.; Smith, M. E.; Stuart, S. N.; Healy, P. C. *J. Phys. Chem.* **1992**, *96*, 7560−7567. (d) Bowmaker, G. A.; Hanna, J. V.; Hart, R. D.; Healy, P. C.; White, A. H. *J. Chem. Soc., Dalton Trans.* **1994**, 2621−2629. (e) Baker, L.-J.; Bowmaker, G. A.; Hart, R. D.; Harvey, P. J.; Healy, P. C.; White, A. H. *Inorg. Chem.* **1994**, *33*, 3925−3931. (f) Wu, G.; Wasylishen, R. E. *Inorg. Chem.* **1996**, *35*, 3113−3116. (g) Hanna, J. V.; Hart, R. D.; Healy, P. C.; Skelton, B. W.; White, A. H. *J. Chem. Soc., Dalton Trans.* **1998**, 2321−2326. (h) Kroeker, S.; Hanna, J. V.; Wasylishen, R. E.; Ainscough, E. W.; Brodie, A. M. *J. Magn. Reson.* **1998**, *135*, 208−215. (i) Bowmaker, G. A.; Effendy; Hanna, J. V.; Healy, P. C.; Reid, J. C.; Rickard, C. E. F.; White, A. H. *J. Chem. Soc., Dalton Trans.* **2000**, 753−762.

(17) (a) Baker, L. J.; Bowmaker, G. A.; Camp, D.; Effendy; Healy, P. C.; Schmidbaur, H.; Steigelmann, O.; White, A. H. *Inorg. Chem.* **1992**, *31*, 3656−3662. (b) Bowmaker, G. A.; Clase, H. J.; Alcock, N. W.; Kessler, J. M.; Nelson, J. H.; Frye, J. S. *Inorg. Chim. Acta* **1993**, *210*, 107−124. (c) Liu, C. W.; Pan, H.; Fackler, J. P., Jr.; Wu, G.; Wasylishen, R. E.; Shang, M. *J. Chem. Soc., Dalton Trans.* **1995**, 3691−3697. (d) Bowmaker, G. A.; Effendy; Harvey, P. J.; Healy, P. C.; Skelton, B. W.; White, A. H. *J. Chem. Soc., Dalton Trans.* **1996**, 2449−2457. (e) Bowmaker, G. A.; Effendy; Harvey, P. J.; Healy, P. C.; Skelton, B. W.; White, A. H. *J. Chem. Soc., Dalton Trans.* **1996**, 2459−2465. (f) Bowmaker, G. A.; Hanna, J. V.; Rickard, C. E. F.; Lipton, A. S. *J. Chem. Soc., Dalton Trans.* **2001**, 20−28. (g) Cingolani, A.; Effendy; Hanna, J. V.; Pellei, M.; Pettinari, C.; Santini, C.; Skelton, B. W.; White, A. H. *Inorg. Chem.* **2003**, *42*, 4938−4948. (h) Effendy; Hanna, J. V.; Marchetti, F.; Martini, D.; Pettinari, C.; Pettinari, R.; Skelton, B. W.; White, A. H. *Inorg. Chim. Acta* **2004**, *357*, 1523−1537.

(18) (a) Angermair, K.; Bowmaker, G. A.; de Silva, E. N.; Healy, P. C.; Jones, B. E.; Schmidbauer, H. *J. Chem. Soc., Dalton Trans.* **1996**, 3121−3129. (b) Baker, L.-J.; Bott, R. C.; Bowmaker, G. A.; Healy, P. C.; Skelton, B. W.; Schwerdtfeger, P.; White, A. H. *J. Chem. Soc., Dalton Trans.* **1995**, 1341−1347. (c) Berners-Price, S. J.; Bowen, R. J.; Hambley, T. W.; Healy, P. C. *J. Chem. Soc., Dalton Trans.* **1999**, 1337−1346. (d) De Silva, E. N.; Bowmaker, G. A.; Healy, P. C. *J. Mol. Struct.* **2000**, *516*, 263−272.

(19) (a) Power, W. P.; Lumsden, M. D.; Wasylishen, R. E. *J. Am. Chem. Soc.* **1991**, *113*, 8257−8262. (b) Lumsden, M. D.; Eichele, K.; Wasylishen, R. E.; Cameron, T. S.; Britten, J. F. *J. Am. Chem. Soc.* **1994**, *116*, 11129−11136. (c) Lumsden, M. D.; Wasylishen, R. E.; Britten, J. F. *J. Phys. Chem.* **1995**, *99*, 16602−16608. (d) Baker, L. J.; Bowmaker, G. A.; Skelton, B. W.; White, A. H. *J. Chem. Soc., Dalton Trans.* **1993**, 3235−3240.

(20) (a) Lindner, E.; Haustein, M.; Mayer, H. A.; Schneller, T.; Fawzi, R.; Steimann, M. *Inorg. Chim. Acta* **1995**, *231*, 201−205. (b) MacFarlane, K. S.; Joshi, A. M.; Rettig, S. J.; James, B. R. *Inorg. Chem.* **1996**, *35*, 7304−7310. (c) Ritleng, V.; Bertani, P.; Pfeffer, M.; Sirlin, C.; Hirschinger, J. *Inorg. Chem.* **2001**, *40*, 5117−5122. (d) Eichele, K.; Nachtigal, C.; Jung, S.; Mayer, H. A.; Lindner, E.; Stroebele, M. *Magn. Reson. Chem.* **2004**, *42*, 807−813. (e) Eichele, K.; Wasylishen, R. E.; Corrigan, J. F.; Doherty, S.; Carty, A. J.; Sun, Y. *Inorg. Chem.* **1993**, *32*, 121−123.

Table 1. Key NMR Data for the Pyrrolyl Group[a]

compound	solvent	^{1}H NMR data	^{13}C NMR data	ref
HNN′	C_6D_6	6.45 (br, 1H), 6.05 (br, 2H)	150.7, 115.9	21, 24
LiNN′	C_6D_6	7.15−7.2 (overlaps with Ar), 6.89 (m, 1 H), 6.42 (m, 1 H)	147.5, 120.7	2, 21
RuCl(NN′)(PCy_3)(=CHPh), **1a**	$CDCl_3$	7.09−7.01 (***H*5**, overlaps with Ar), 6.51 (br, 1 H, ***H*3**), 6.18 (dd, ^3J = 3.9, 1.6 Hz, 1 H, ***H*4**)	142.8 (d, $^3J_{CP}$ = 2.0 Hz, ***C*2**), 141.7 (s, ***C*3**), 120.2 (s, ***C*5**), 114.0 (s, ***C*4**)	2
RuCl(NN′)($py)_2$(=CHPh), **1b**	$CDCl_3$	8.59−6.91 (***H*3**, overlaps with Ar), 6.46 (br, 1 H, ***H*3**), 6.20 (m, 1 H, ***H*4**)		2
RuCl(η^5-C_5H_4N)($PPh_3)_2$, **2a**	C_6D_6	5.61 (2H), 4.24 (2H)	108.4, 82.7	3
RuH(η^5-C_5H_4N)($PPh_3)_2$, **2b**	C_6D_6	5.33 (2H), 5.03 (2H)	110.0, 82.0	3
[RuCl(NN′)($PPh_3)_2]_2$, **3b**	C_6D_6	7.15 (br s, 1 H, ***H*5**), 6.34 (m, 1 H, ***H*4**), 6.18 (br s, 1H, ***H*3**)	147.5 (s, **C2**), 143.7 (s, ***C*3**), 121.3 (s, ***C*5**), 114.5 (s, ***C*4**)	this work

[a] Chemical shifts in ppm, coupling constants in Hz. Assignments (where reported) shown in bold face; atom numbering standardized to that of Scheme 1.

Scheme 1

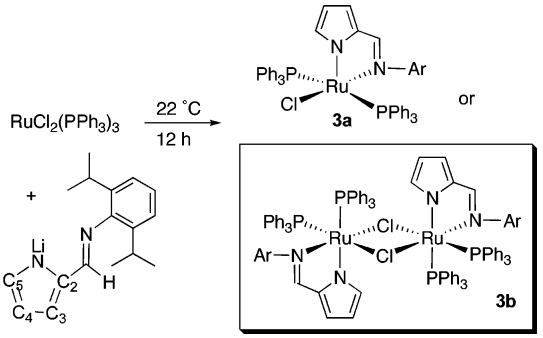

Results and Discussion

Reaction of $RuCl_2(PPh_3)_3$ with LiNN′ in dichloromethane effects complete conversion to a single species (**3**) within 12 h at room temperature (Scheme 1). Isolated yields are limited to ca. 72% by the high solubility of the product in all solvents, including pentane. The presence of two PPh_3 groups on the Ru center(s) is inferred from observation (^{1}H NMR) of a triplet for the azomethine proton (7.90 ppm; t, $^4J_{HP}$ = 2.1 Hz), which collapses to a singlet when phosphorus decoupling is applied. The isopropyl groups give rise to two sets of methyl signals (^{1}H, ^{13}C NMR), suggesting restricted rotation about each aryl−methine C−C bond. The chemical shifts of the proton and carbon nuclei in the pyrrolyl ring can provide key insight into the bonding mode and hapticity of the ring, strong upfield shifts being characteristic of π-bound[3] pyrrole (Table 1). We thus undertook analysis by COSY, HMQC, and HMBC correlation experiments to deconvolute the signals due to the pyrrolide ring from those due to the PPh_3 or NAr groups. The azomethine proton provides a convenient starting point, permitting location of the signals due to C2 and C3 (HMBC; C2 is the imine-functionalized pyrrole carbon). We distinguish these on the basis of the C3−H3 coupling (HMQC): in turn, this permits assignment of signals for H4 (COSY) and C4 (HMQC), following which the peaks for H5 and C5 are located from their COSY and HMQC correlations, respectively. Chemical shifts for the pyrrole ring protons are in good agreement with values reported for coordinatively saturated κ^2-iminopyrrole complexes,[21−24] and are little perturbed relative to values for the parent lithium salt, as expected for a σ-coordinated pyrrolide unit. The ^{13}C NMR data likewise agree with literature values for the NN′-chelate complexes, showing little sensitivity to the identity of the metal or ancillary ligands. In comparison, resonances for the π-bound pyrrolide in **2** are shifted upfield by 1−2 (^{1}H NMR) or 30 ppm (^{13}C NMR).[3]

The presence of a sharp singlet at 58.5 ppm in the solution ^{31}P{^{1}H} NMR spectrum of **3** at room temperature, the triplet multiplicity of the azomethine proton resonance, and the integration values for the aromatic region in the ^{1}H NMR spectrum all point toward the presence of two equivalent triphenylphosphine ligands, as in structure **3a**. (We locate the pyrrolide nitrogen in the apical site of this square pyramidal structure, rather than the imine nitrogen, in view of the higher trans influence expected for this anionic ligand). Unexpectedly, however, we observe partial resolution of the ^{31}P NMR singlet on cooling to −90 °C (C_7D_8). Two broad peaks emerge at 71.8 and 46.8 ppm ($\nu_{0.5}$ = 110 and 99 Hz, respectively), suggesting the alternative possibility of structure **3b**, although their singlet multiplicity implies rapid exchange of the inequivalent phosphorus centers even at −90 °C. (Site exchange is presumably mediated by reversible opening of the dative chloride bond(s) in the edge-bridged structure, as no correlation between the signals for free and bound PPh_3 is found in ^{31}P EXSY correlation experiments in the presence of 5 equiv of PPh_3). MALDI experiments did not enable us to distinguish between the mono- and diruthenium possibilities: cations corresponding to monomeric and dimeric species (albeit with some fragmentation in the latter case) were observed, but these could arise from cleavage or agglomeration processes, respectively. To clarify this point, we carried out ^{1}H PGSE diffusion NMR measurements (Figure 1) to gain insight into molecular size and nuclearity. Such experiments have proved invaluable in establishing the extent of aggregation in other systems, including a number of mononuclear and dinuclear ruthenium complexes.[25] A translational diffusion constant of 6.04 ×

(21) Dawson, D. M.; Walker, D. A.; Thornton-Pett, M.; Bochmann, M. *J. Chem. Soc., Dalton Trans.* **2000**, 459−466.
(22) Hao, H.; Bhandari, S.; Ding, Y.; Roesky, H. W.; Magull, J.; Schmidt, H.-G.; Noltemeyer, M.; Cui, C. *Eur. J. Inorg. Chem.* **2002**, 1060−1065.
(23) (a) Matsuo, Y.; Mashima, K.; Tani, K. *Organometallics* **2001**, *20*, 3510−3518. (b) Matsuo, Y.; Mashima, K.; Tani, K. *Chem. Lett.* **2000**, 1114−1115.
(24) Sasabe, H.; Nakanishi, S.; Takata, T. *Inorg. Chem. Commun.* **2003**, *6*, 1140−1143.

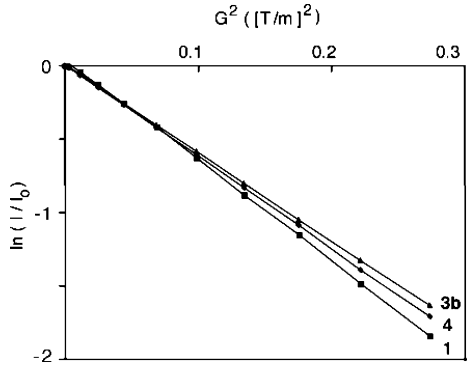

Figure 1. ^{1}H PGSE diffusion measurements for **3b**, vs **1a** and **4** ($CDCl_3$, 15 mM; 295 K). The slopes of the lines are related to the translational diffusion constants (see Experimental Section).[27]

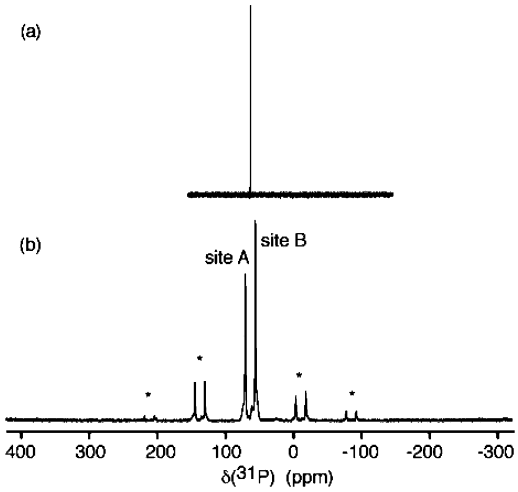

Figure 2. $^{31}P\{^1H\}$ NMR spectra of **3b** (22 °C). (a) Solution spectrum (C_6D_6, 7.05 T). (b) Solid-state CP/MAS spectrum (4.7 T; MAS rate = 5.3 kHz). Pairs of spinning sidebands are marked with asterisks. Fine structure at the base of the peaks is due to $J(^{99}Ru,^{31}P)$ coupling: see text.

10^{-10} m^2 s^{-1} was measured for **3b**, vs values of 6.30×10^{-10} m^2 s^{-1} for dinuclear RuCl(dcypb)(μ-Cl)$_3$Ru(dcypb)(N_2), **4** (dcypb = 1,4-bis(dicyclohexylphosphino)butane),[26] and 6.86×10^{-10} m^2 s^{-1} for mononuclear **1a** (all values $\pm$ <0.5%, consistent with literature precedents).[25] The smaller diffusion constant for **3b** is consistent with a dimeric structure.

A series of solid-state NMR experiments was carried out in order to gain more detailed insight into the structure of **3**. Figure 2 shows the solution and solid-state (CP/MAS) $^{31}P\{^1H\}$ NMR spectra. Two magnetically inequivalent sites are resolved at room temperature in the solid state, with isotropic chemical shifts of 66.8 and 52.1 ppm. Their averaged value is nearly identical to that observed in solution at ambient temperatures (59.5 ppm vs 58.5 ppm); solvent and crystal packing effects account for the small difference in these values. The presence of two resolved isotropic ^{31}P resonances in the solid state indicates the presence of at least two magnetically inequivalent sites in the asymmetric unit of the crystal structure. The isotropic resonances are flanked by a series of spinning sidebands spaced at integer multiples of the MAS frequency. Their large span (~200 ppm) suggests substantial anisotropy of the phosphorus chemical shift tensor, as discussed in more detail below.

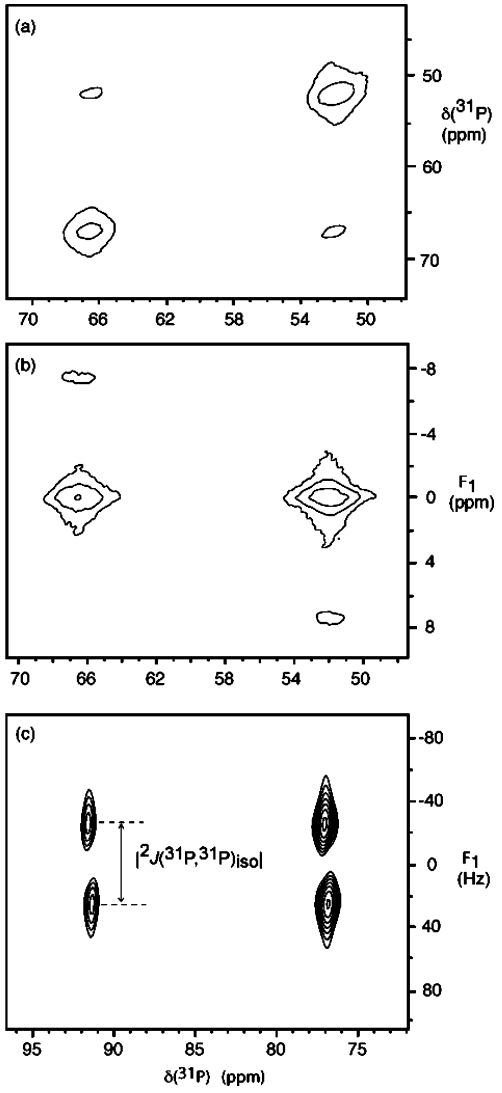

Figure 3. Solid-state NMR spectra of **3b**. (a) $^{31}P-^{31}P$ CP/COSY. (b) ^{31}P CP/SECSY (4.7 T; MAS rate 5.3 kHz). (c) CP 2D *J*-resolved NMR spectrum (11.75 T; MAS rate = 5.0 kHz), showing the first-order spinning sidebands for each of the two inequivalent ^{31}P sites.

The through-bond connectivity of the two inequivalent ^{31}P nuclei was established by COSY and SECSY correlation experiments (Figure 3a,b). The off-diagonal peaks in the COSY spectrum, as well as the correlations above and below the zero-frequency ($F_1 = 0$) axis in the SECSY spectrum, indicate indirect nuclear spin−spin coupling. The 2D *J*-resolved spectrum (Figure 3c), which measures isotropic $^{31}P-^{31}P$ indirect nuclear spin−spin coupling constants ($J(^{31}P,^{31}P)_{iso}$),[11b,d] indicates that the two ^{31}P resonances arise from the same compound, rather than different polymorphs in the same sample. Correlations are shown for the +1 spinning sideband. The magnitude of the *J* value along the F_1 axis, $|^2J_{PP}| = 52 \pm 5$ Hz, is consistent with cis-disposition

(25) Leading references: (a) Pregosin, P. S.; Kumar, P. G. A.; Fernandez, I. *Chem. Rev.* **2005**, *105*, 2977−2998. (b) Fernandez, I.; Pregosin, P. S.; Albinati, A.; Rizzato, S. *Organometallics* **2006**, *25*, 4520−4529. (c) Goicoechea, J. M.; Mahon, M. F.; Whittlesey, M. K.; Kumar, P. G. A.; Pregosin, P. S. *Dalton Trans.* **2005**, 588−597. (d) Kumar, P. G. A.; Pregosin, P. S.; Goicoechea, J. M.; Whittlesey, M. K. *Organometallics* **2003**, *22*, 2956−2960. (e) Zuccaccia, D.; Macchioni, A. *Organometallics* **2005**, *24*, 3476−3486.

(26) Amoroso, D.; Yap, G. P. A.; Fogg, D. E. *Can. J. Chem.* **2001**, *79*, 958−963.

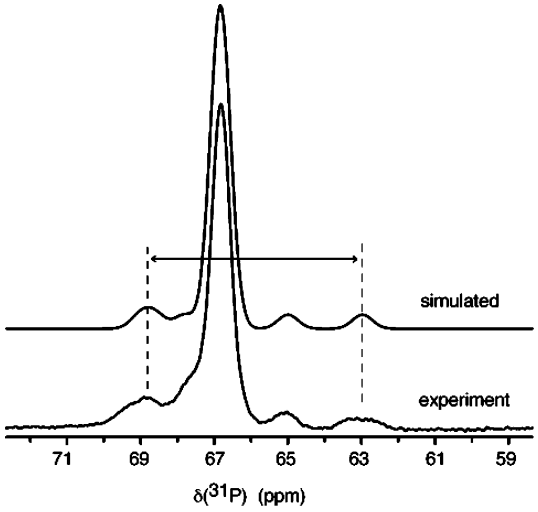

Figure 4. Solid-state ^{31}P CP/MAS NMR centerband of one of the two ^{31}P sites in **3b** (11.75 T; all sidebands summed into the centerband to approximate an infinite-MAS-rate spectrum). The simulated spectrum is generated using the parameters summarized in Table 2. The arrow denotes a splitting of five times the value of the isotropic $^1J(^{99}\text{Ru},^{31}\text{P})$ coupling constant.

of the inequivalent phosphine ligands.[28] Solid-state values of $|^2J_{PP}|$ show the trend familiar from solution studies, with cis-disposed phosphines giving values approximately one-tenth of those found for trans-phosphines. Thus, values of 39 ± 4 and 58 ± 5 Hz for the cis-^{31}P nuclei in $RuCl_2(\eta^1\text{-}Ph_2PCH_2CH_2OCH_3)_2(\eta^2\text{-en})$ (en = ethylenediamine)[20d] and $RhCl(PPh_3)_3$,[11b] respectively, compare with typical values for trans phosphines of 366 Hz in $RhCl(PPh_3)_3$,[11b] 334 Hz in *t*-$Ni(SCN)_2(DMPP)_2$ (DMPP = 1-phenyl-3,4-dimethylphosphole),[7] and 530 Hz in *t*-$PdCl_2(DBP)_2$ (DBP = 5-phenyldibenzophosphole).[7]

The bases of the peaks in Figure 2b reveal fine structure due to $^1J(^{99}\text{Ru},^{31}\text{P})_{iso}$ coupling. Shown in Figure 4 is a more detailed view of the isotropic resonance (reconstructed by adding in the intensity of all spinning sidebands) for one of the two phosphorus sites ("site A"). The dominant peak, at 66.8 ppm, arises from ^{31}P nuclei adjacent to spin-0 ruthenium isotopes, or isotopes that are self-decoupled from ^{31}P. The fine structure, due to the 12.8% natural abundance of ^{99}Ru ($I = 5/2$), consists of six peaks, with the difference between the highest and lowest field signals (1218 Hz) corresponding to five times the isotropic $J(^{99}\text{Ru},^{31}\text{P})$ coupling constant. The magnitude of $^1J(^{99}\text{Ru},^{31}\text{P})$ is thus 244 Hz. To our knowledge, this is one of the largest ruthenium−phosphorus coupling constants measured to date; previously reported values range between 100 and 174 Hz.[20e] No evidence is observed for coupling between ^{101}Ru and ^{31}P, consistent with self-decoupling of ^{101}Ru from ^{31}P, a function of the larger nuclear electric quadrupole moment of ^{101}Ru compared with ^{99}Ru ($Q(^{101}\text{Ru})/Q(^{99}\text{Ru}) = 5.78$).

The details of the simulation of the spectrum of a spin-1/2 nucleus (^{31}P) coupled to a half-integer quadrupolar nucleus (^{99}Ru) under MAS have been discussed extensively.[29] Briefly, in the solid state, the Zeeman states of the quadrupolar ^{99}Ru nucleus are perturbed by the quadrupolar interaction; as a result of breakdown of the high-field approximation, dipolar interactions between ^{99}Ru and ^{31}P are not completely averaged by MAS. The residual dipolar coupling, *d*, depends on the ^{99}Ru nuclear quadrupolar coupling constant (C_Q), the asymmetry parameter of the ^{99}Ru electric field gradient (EFG) tensor (η), the effective direct dipolar coupling between ^{99}Ru and ^{31}P (R_{eff}), the orientation of the dipolar vector in the principal axis system (PAS) of the EFG tensor (described by the polar angles α and β), and the Larmor frequency of ^{99}Ru (ν_{Ru}):

$$d = -\frac{3C_Q R_{eff}}{20\nu_{Ru}}[(3\cos^2\beta - 1) + \eta\sin^2\beta\cos 2\alpha] \quad (1)$$

It is well known that $R_{eff} = R_{DD} - \Delta J/3$, where R_{DD} is the direct dipolar coupling between two nuclei ($\mu_0\hbar\gamma_1\gamma_2\langle r_{12}^{-3}\rangle/8\pi^2$) and ΔJ is the anisotropy in their indirect nuclear spin−spin coupling tensor. We make the standard assumption that $R_{DD} \gg \Delta J/3$; in the absence of independent measurement of the Ru−P internuclear distance, we cannot conclude that ΔJ is significantly different from zero given the errors associated with measurement of *d*. We infer the magnitude of $C_Q(^{99}\text{Ru})$, with the help of some reasonable assumptions. For an axially symmetric ^{99}Ru EFG tensor, and using our experimental value of $d = -140$ Hz at 11.75 T, we find that the value of $C_Q(^{99}\text{Ru}) \approx -57$ MHz if the largest component of the EFG tensor (V_{ZZ}) lies along the Ru−P bond. This is only an approximate value, however, since there is no reason to presume that V_{ZZ} lies preferentially along one of the two nonequivalent Ru−P bonds. Our approximate value (though somewhat larger) is of the same order of magnitude as a previously estimated value of $C_Q(^{99}\text{Ru}) \approx -17$ MHz, which was obtained using analogous assumptions in the interpretation of ^{31}P MAS NMR spectra of solid *ttt*-$Ru(CCPh)_2(CO)_2(PEt_3)_2$.[20e]

Further insight into the electronic structure about the phosphorus nuclei in **3b** was obtained from ^{31}P dipolar-chemical shift spectra[30] recorded on powdered samples under stationary conditions at two different applied magnetic field strengths (Figure 5). These spectra contain information on the two different phosphorus chemical shift tensors and their orientations relative to the ^{31}P−^{31}P dipolar vector. The

(27) The PGSE technique, involving application of two equal pulsed field gradients, causes attenuation of NMR signals to an extent determined by the rate of translational diffusion of the nuclei under observation. The magnitude of the diffusion constant correlates with the hydrodynamic radius of the molecule. See: Stilbs, P. *Prog. Nucl. Magn. Reson. Spectrosc.* **1987**, *19*, 1−45; see also ref 25 (a).

(28) Verkade, J.-G.; Quin, L.-D. Phosphorus-31 NMR Spectroscopy in Stereochemical Analysis: Organic Compounds and Metal-Complexes. In *Methods in Stereochemical Analysis*; VCH Publishers: Deerfield Beach, FL; 1987; Vol. 8.

(29) (a) Hexem, J. G.; Frey, M. H.; Opella, S. J. *J. Chem. Phys.* **1982**, *77*, 3847−3856. (b) Olivieri, A. C.; Frydman, L.; Diaz, L. E. *J. Magn. Reson.* **1987**, *75*, 50−62. (c) Olivieri, A.; Frydman, L.; Grasselli, M.; Diaz, L. *Magn. Reson. Chem.* **1988**, *26*, 615−618. (d) Olivieri, A. C. *J. Magn. Reson.* **1989**, *81*, 201−5. (e) Grasselli, M.; Diaz, L. E.; Olivieri, A. C. *Spectrosc. Lett.* **1991**, *24*, 895−907. (f) Eichele, K.; Wasylishen, R. E. *Solid State Nucl. Magn. Reson.* **1992**, *1*, 159−163. (g) Gan, Z.; Grant, D. M. *J. Magn. Reson.* **1990**, *90*, 522−534. (h) Harris, R. K.; Olivieri, A. C. *Prog. Nucl. Magn. Reson. Spectrosc.* **1992**, *24*, 435−456. (i) Eichele, K.; Wasylishen, R. E. *Inorg. Chem.* **1994**, *33*, 2766−2773.

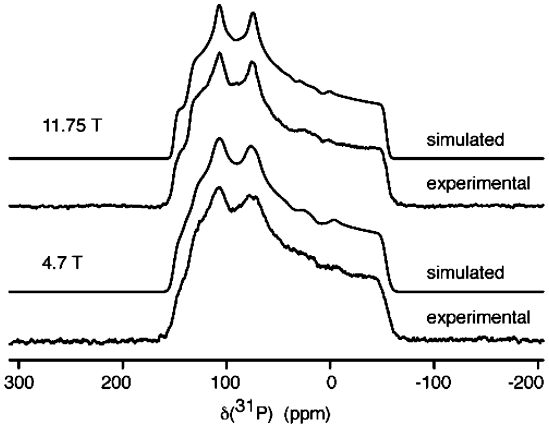

Figure 5. Solid-state ^{1}H-decoupled ^{31}P dipolar-chemical shift NMR spectra of **3b** obtained with CP under stationary conditions (11.75 and 4.7 T). Simulated spectra produced using the parameters of Table 2 and the WSOLIDS1 software package.

Table 2. Summary of ^{31}P NMR Parameters for **3b**, from 1D and 2D ^{31}P Solid-State NMR Experiments

	site A	site B
δ_{iso}[a] (ppm)	66.8 ± 0.5	52.1 ± 0.5
δ_{11} (ppm)	149.8 ± 1.0	136.0 ± 1.0
δ_{22} (ppm)	107.0 ± 1.0	75.0 ± 1.0
δ_{33} (ppm)	−55.0 ± 1.0	−53.5 ± 1.0
Ω (ppm)	205.5	189.5
κ	0.58	0.36
α[b] (°)	64 ± 10	0 ± 10
β (°)	41 ± 10	−56 ± 10
γ (°)	35 ± 20	105 ± 20
R_{eff}(^{31}P, ^{31}P) (Hz)	660 ± 50	
^2J(^{31}P, ^{31}P)$_{iso}$ (Hz)	52 ± 5	
^1J(^{99}Ru, ^{31}P)$_{iso}$ (Hz)	244 ± 20	*c*
d(^{99}Ru, ^{31}P) (Hz)	−140 ± 15	*d*

[a] Obtained from the 1D MAS NMR spectra. [b] The angles α, β, and γ define the orientations required to rotate the ^{31}P−^{31}P dipolar tensor into the chemical shift tensor PAS. The value of α for site B was arbitrarily set to zero, as only the difference affects the observed dipolar-chemical shift spectrum. [c] Splitting due to ^1J(^{99}Ru,^{31}P) is not as well resolved for site B; however, the pattern is consistent with a coupling constant similar to that found for site A. [d] Splitting due to ^1J(^{99}Ru,^{31}P) is not as well resolved for site B; however, the sense of the coupling pattern is opposite to that found for site A (Figure 4), implying a significant difference in the orientation of the Ru−P dipolar vector relative to the ^{99}Ru EFG principal axis system.

simulations are based on the assumption of an effectively isolated spin-1/2 pair; very small discrepancies could arise from the fact that we are ignoring coupling to $^{99/101}$Ru, as well as nearby $^{35/37}$Cl nuclei. However, the high quality of the simulations tends to suggest that the isolated spin-pair assumption is valid. The parameters resulting from the spectral simulations are summarized in Table 2. The effective ^{31}P,^{31}P dipolar coupling constant, 660 ± 50 Hz, is consistent with a through-space ^{31}P−^{31}P separation of ∼3.1 Å, providing further evidence for mutually cis phosphine ligands in the solid state.

The data summarized for **3b** represent only the second set of ^{31}P chemical shift tensor magnitudes reported for octahedral ruthenium phosphine compounds. The first such values were reported in 2004 in a detailed study of solid $RuCl_2(\eta^1\text{-}Ph_2PCH_2CH_2OCH_3)_2(\eta^2\text{-en})$ by Eichele et al., in which δ_{11} ranged from 95 to 109 ppm, δ_{22} from 56 to 76 ppm, and δ_{33} from −75 to −60 ppm for the five resolvable ^{31}P sites.[20d] The most striking difference between these values and those herein is in the magnitude of the least-shielded component, δ_{11}, which is 136.0 and 149.8 ppm for each of the two sites in **3b**. From the spectral simulations, we also find that the most shielded components (δ_{33}) of the two phosphorus chemical shift tensors are at 79° relative to one another, suggesting that this component lies approximately along the Ru−P bond for each phosphorus site. The supposition that the δ_{33} component lies close to the direction of the phosphorus−metal bond in metal−phosphine complexes is consistent with the conclusions of related studies;[7] however, this does not appear to be a general rule.[15a,b]

Conclusions

The foregoing describes the use of an iminopyrrolato group as a pseudohalide ligand within an edge-bridged ruthenium dimer containing cis-disposed triphenylphosphine ligands. The stability of **3b** against $\sigma \rightarrow \pi$ isomerization, despite the ease with which the required coordination sites could be generated by loss of a dative chloride donor, provides good evidence for the stability of the σ-pyrrolide donor within this five-membered chelate ring. Solid-state NMR analysis proved invaluable in elucidating the cis orientation of the triphenylphosphine groups in **3b**. In the course of this analysis, we have measured what appears to be the largest ruthenium−phosphorus spin−spin coupling constant yet reported in solution or the solid state. This highlights the relative scarcity of solid-state NMR information concerning hexacoordinate ruthenium complexes. Further investigation with related compounds, including pyrrolide-based pseudohalide catalysts relevant to olefin metathesis, is under way and will be reported in due course.

Experimental Section

All reactions were carried out at 22 °C under N_2 using standard Schlenk and drybox techniques. Dry, oxygen-free solvents were obtained using a Glass Contour solvent purification system, and stored over Linde 4 Å molecular sieves. Deuterated solvents were obtained from Cambridge Isotope Laboratories Ltd. $CDCl_3$ was refluxed over and distilled from CaH_2 under an atmosphere of N_2. C_6D_6 was dried over activated sieves (Linde 4 Å) and degassed by consecutive freeze−pump−thaw cycles. Ampoules of toluene-d_8 were used as received. $RuCl_2(PPh_3)_3$,[31] 2-[(2,6-diisopropylphenyl)-imino]pyrrole (HNN′),[21] RuCl(NN′)(PCy_3)(CHPh) (**1a**),[2] and RuCl-(dcypb)(μ-Cl)$_3$Ru(dcypb)(N_2) (**4**)[26] were prepared according to literature procedures. Routine solution ^{1}H NMR (300 MHz), ^{31}P NMR (121 MHz), and ^{13}C NMR (75 MHz) spectra were recorded on a Bruker Avance-300 spectrometer. NMR spectra are reported in ppm relative to external 85% H_3PO_4 (^{31}P) or TMS (^{1}H, ^{13}C) at 0 ppm. PGSE NMR measurements were recorded on a Bruker Avance-500 spectrometer. Solid state ^{31}P NMR analysis of powdered samples of **3b** were performed at 4.7 (81.0 MHz) and 11.75 T (202.47 MHz) using Bruker ASX and Avance consoles,

(30) (a) VanderHart, D. L.; Gutowsky, H. S. *J. Chem. Phys.* **1968**, *49*, 261−271. (b) VanderHart, D. L.; Gutowsky, H. S.; Farrar, T. C. *J. Chem. Phys.* **1969**, *50*, 1058−1065. (c) Linder, M.; Hoehener, A.; Ernst, R. R. *J. Chem. Phys.* **1980**, *73*, 4959−4970. (d) Eichele, K.; Wasylishen, R. E. *J. Magn. Reson. A* **1994**, *106*, 46−56.

(31) Hallman, P. S.; Stephenson, T. A.; Wilkinson, G. *Inorg. Synth.* **1970**, *12*, 237−240.

respectively. Inert-atmosphere MALDI-TOF analysis was performed using a Bruker OmniFlex MALDI-TOF spectrometer equipped with a nitrogen laser (337 nm) and interfaced to a MBraun glovebox. Data were collected in positive reflectron mode, with the accelerating voltage held at 20 kV. Pyrene matrix and analyte solutions were prepared in CH_2Cl_2 at concentrations of 20 and 1 mg/mL, respectively. Samples were mixed in a matrix/analyte ratio of 20:1. Microanalyses were carried out by Guelph Chemical Laboratories Ltd., Guelph, Ontario.

Lithium 2-[(2,6-Diisopropylphenyl)imino]pyrrolide (LiNN′). In a modification of the literature method,[21] LiNN′ was obtained free of a solvating molecule of diethyl ether[2] by addition of *n*-BuLi (5.5 mL, 8.85 mmol) in 2 mL of hexanes to a solution of HNN′ (1.84 g, 7.25 mmol) in 40 mL of hexanes at −80 °C. The reaction mixture was stirred at −80 °C for 2 h then stripped of solvent to yield an off-white solid, which was extracted with hexanes (10 mL). Yield: 1.4 g (74%). The product was stored at −35 °C under N_2. ^{1}H NMR (C_6D_6, δ): 8.02 (br s, 1 H, N=C*H*), 7.40−7.15 (br m, 4 H, Ar + pyr), 6.89 (br m, 1 H, pyr), 6.42 (br m, 1 H, pyr), 3.42 (sept, $^3J_{HH}$ = 7 Hz, 2 H, 2 × C*H*Me$_2$), 1.12 (d, $^3J_{HH}$ = 7 Hz, 12 H, 4 × C*H*$_3$).

[RuCl(κ^2-*N*,*N*′-ArN=CHC$_4$H$_3$N)(PPh$_3$)$_2$]$_2$ (3b); Ar = 2,6-^{i}Pr$_2$C$_6$H$_3$. Addition of solid LiNN′ (626 mg, 2.40 mmol) to a dark brown solution of $RuCl_2(PPh_3)_3$ (1.27 g, 1.30 mmol) in CH_2Cl_2 (30 mL) resulted in a color change to black. (We earlier noted[2] the requirement for excess LiNN′, imposed by competing protonation to yield HNN′). Stirring was continued for 12 h, after which the solvent was removed in vacuo. The resulting black, oily solid was dissolved in 10 mL of hexanes and chilled to −30 °C to afford a dark purple precipitate. This was filtered cold, washed with cold hexanes (3 × 10 mL), and dried in vacuo. Yield: 1.7 g (72%). Low yields are incurred by the high solubility of **3b** in all hydrocarbon solvents, including pentane. ^{31}P{^{1}H} NMR (C_6D_6, δ): 58.5 (s, *P*Ph$_3$). ^{1}H NMR (C_6D_6, δ): 7.90 (t, $^4J_{HP}$ = 2.1 Hz, 1 H, N=C*H*), 7.29−6.85 (m, 33 H, Ph, Ar), 7.15 (br s, 1 H, pyr *H*$_5$), 6.34 (m, 1 H, pyr *H*$_4$), 6.18 (br s, 1H, pyr *H*$_3$), 2.48 (sept, $^3J_{HH}$ = 7 Hz, 2 H, 2 × C*H*Me$_2$), 0.90 (d, $^3J_{HH}$ = 7 Hz, 6 H, 2 × C*H*$_3$), 0.83 (d, $^3J_{HH}$ = 7 Hz, 6 H, 2 × C*H*$_3$). ^{13}C{^{1}H} NMR (C_6D_6, δ): 164.2 (s, N=*C*H), 147.5 (s, pyr *C*$_2$), 144.1 (s, Ar *C*$_1$), 143.7 (s, pyr *C*$_3$), 143.0 (s, Ar *C*$_2$, *C*$_6$),135.0−135.5 (multiple s, Ph), 126.8 (s, Ar *C*$_5$), 123.4 (s, Ar *C*$_3$, *C*$_5$), 121.3 (s, pyr *C*$_4$), 114.5 (s, pyr *C*$_4$), 29.4 (s, *C*HMe$_2$), 26.5 (s, *C*H$_3$), 22.7 (s, *C*H$_3$). Anal. Calcd for $C_{106}H_{102}Cl_2N_4P_4Ru_2$: C, 69.61; H, 5.62; N, 3.06%. Found C, 69.12; H, 5.67; N, 2.79%. MALDI-TOF MS, *m*/*z*: Calcd for $[Ru_2Cl_2(NN')_2(PPh_3)_4]^{+\bullet}$, 1828.5; Found, 1044.2 (corresponds to $[M - 3PPh_3 + 2H]^+$). Calcd for $[RuCl(NN')(PPh_3)]^{+\bullet}$: 652.1; Found, 652.3.

PGSE NMR Measurements. ^{1}H PGSE NMR measurements were performed in $CDCl_3$ (15 mM, 22 °C) on a Bruker Avance-500 spectrometer using the standard Stejskal−Tanner spin−echo pulse sequence,[27] with a 4 ms gradient duration (δ) and an intergradient spacing (Δ) of 10 ms, ramping the gradient strength (G) in 10% increments from 0% to 100%, or 8.51×10^{-4} to 0.524 T m^{-1}. Values of the diffusion constant, D, were calculated from the experimentally derived line intensities I (I_0 = intensity at zero gradient strength) according to eq 2, using a value of 2.675×10^8 T^{-1} s^{-1} for the gyromagnetic ratio (γ) of the ^{1}H nucleus. All spectra were acquired using 16 scans and 64K points, with a spectral width of 7440 Hz, and processed with exponential line broadening of 1 Hz. D values were calculated from the three most intense lines in each spectrum; standard deviations ranged from 0.026 to 0.062 × 10^{-10} m^2 s^{-1} (0.3−0.9%), in keeping with literature precedents.[25]

$$\ln\left(\frac{I}{I_o}\right) = -(\gamma\delta)^2 G^2 \left(\Delta - \frac{\delta}{3}\right) D \qquad (2)$$

Solid-State NMR Spectroscopy. ^{31}P NMR spectra of powdered samples of **3b** were obtained at 4.7 (81.0 MHz for ^{31}P) and 11.75 T (202.47 MHz for ^{31}P) using Bruker ASX and Avance consoles, respectively. For experiments at 4.7 T, custom Teflon inserts were packed under nitrogen in a glovebox and placed inside zirconia rotors (7 mm o.d.) for use in a Bruker double-resonance MAS probe. For experiments at 11.75 T, zirconia rotors of 4 mm o.d. were used in a Bruker triple-resonance MAS probe. ^{31}P NMR chemical shifts were indirectly referenced to external 85% H_3PO_4 at 0 ppm by using solid ammonium dihydrogen phosphate as a secondary reference at δ_P = +0.81 ppm.[32] All ^{31}P NMR spectra were obtained using cross-polarization (CP) from ^{1}H, and FIDs were recorded with high-power proton decoupling. Typical proton $\pi/2$ pulses were 4.0−4.5 μs at 4.7 T and 3.0−3.3 μs at 11.75 T. Typical CP contact times were 2−3 ms, and typical recycle delays were 10 s. Regular CP experiments and standard MAS probes were used for recording spectra of stationary samples. 1D data were processed (exponential multiplication, zero-filling) using Bruker's XWinNMR software. Spectral simulations were performed using WSOLIDS1.[33]

Two-dimensional ^{31}P−^{31}P correlation spectroscopy (COSY), spin−echo correlation spectroscopy (SECSY), and *J*-resolved spectroscopy experiments[11b,d] were performed at 4.7 T; 2D *J*-resolved spectra were also obtained at 11.75 T. The pulse sequences for these experiments may be summarized as CP-t_1-π/2(^{31}P)-ACQ-(t_2) (COSY); CP-t_1/2-π/2(^{31}P)-t_1/2-ACQ (SECSY); CP-t_1/2-π(^{31}P)-t_1/2-ACQ (*J*-resolved). The phase cycling used is given by Wu and Wasylishen.[11d] All 2D experiments were recorded in a rotor-synchronized fashion, e.g., for *J*-resolved experiments at 11.75 T and at an MAS rate of 5 kHz, the t_1 increment was set to 200 μs. Typically, 128 or 256 t_1 increments were used. An MAS rate of 5.3 kHz was used for 2D experiments recorded at 4.7 T. Data were apodized by a cosine function in the directly detected dimension and by a squared cosine function in the indirect dimension. The resulting data were zero-filled at least once in each dimension, followed by 2D Fourier transformation, and displayed in magnitude mode. All two-dimensional datasets were processed and analyzed using nmrPipe.[34]

Acknowledgment. Dr. Klaus Eichele (Universitat Tübingen) is thanked for generously providing copies of the two-dimensional pulse sequences used in this work and for helpful discussions. We thank Dr. Glenn Facey (NMR Facility Manager) for his technical assistance and expertise and NSERC (D.E.F., D.L.B.) and the University of Ottawa Faculty of Science (D.L.B.) for funding.

IC061021I

(32) Bryce, D. L.; Bernard, G. M.; Gee, M.; Lumsden, M. D.; Eichele, K.; Wasylishen, R. E. *Can. J. Anal. Sci. Spectrosc.* **2001**, *46*, 46−82.
(33) Eichele, K., Wasylishen, R. E. *WSOLIDS NMR Simulation Package*, 1.17.30; Dalhousie University: Halifax, Canada, 2001.
(34) Delaglio, F.; Grzesiek, S.; Vuister, G. W.; Zhu, G.; Pfeifer, J.; Bax, A. *J. Biomol. NMR* **1995**, *6*, 277−293.